Catalysis Today 139 (2008) 168–173

Contents lists available at ScienceDirect

Catalysis Today

journal homepage: www.elsevier.com/locate/cattod

NO reduction by CO over gold based on ceria, doped by rare earth metals

Lyuba Ilieva [a,*], Giuseppe Pantaleo [b], Ivan Ivanov [a], Radka Nedyalkova [a], Anna Maria Venezia [b], Donka Andreeva [a]

[a] Institute of Catalysis, BAS, "Acad. G. Bonchev" Street, bl.11, 1113 Sofia, Bulgaria
[b] Istituto per lo Studio di Materiali Nanostrutturati, CNR, Via Ugo La Malfa, I-90146 Palermo, Italy

ARTICLE INFO

Article history:
Available online 15 October 2008

Keywords:
Gold catalysts
Doped ceria
La
Sm
Gd
Y dopants
NO reduction by CO
Selectivity
Influence of water

ABSTRACT

The reduction of NO by CO over gold catalysts supported on ceria doped by rare earth metals (Y, La, Sm and Gd) was studied. The mixed oxide supports, containing 10 wt% of the dopant, were prepared by co-precipitation and then 2 wt% gold was loaded by deposition–precipitation method. Gold catalysts, supported on lanthanides doped ceria showed a high activity and stability. The conversions both of NO and CO at 250 °C were close to 100% using Sm, La or Gd as dopants. Below 250 °C the Au catalyst on Sm doped ceria exhibited a little higher activity. The lowest catalytic activity was observed using Y as a modifier. The lattice parameter *a* of ceria and the average size of ceria crystallites were evaluated by XRD. The defective structure of ceria, including oxygen vacancies, caused by the introduction of Me^{3+} dopant, was estimated by Raman spectroscopy data. The redox behaviour of fresh gold samples as well as after their reoxidation at 220 °C was established by TPR technique. The low temperature reducibility of the reoxidized gold catalysts supported on doped CeO_2 showed a good correlation with the catalytic properties. It was established that the addition of water to the gas feed improved the catalysts' selectivity to N_2.

1. Introduction

Metal over ceria catalysts are several orders of magnitude more active than metals over alumina or other oxide supports in a number of redox reactions [1–3]. Metal-doped ceria has a higher oxygen storage capacity (OSC) and better reducibility than pure ceria [4–6]. The addition of different metal dopants with valences lower than (4+) to CeO_2 leads to the formation of oxygen vacancies in the ceria structure [7,8]. The involving of two trivalent ions in CeO_2 should lead to one oxygen vacancy generated to balance the charge. The counting, in fact, is not so simple, as there are intrinsic oxygen vacancies in undoped ceria and their concentration may change to some extent upon additives doping [9]. In our previous papers [10,11], we have studied the addition of Al^{3+} to ceria, which increases the oxygen vacancies formation, as well as the stability of gold and ceria particles against agglomeration during the catalytic tests of NO reduction by CO. Gold catalysts based on ceria are very promising for different applications, like CO and hydrocarbons oxidation, WGS reaction, reduction of NO_x by CO and hydrocarbons, etc. NO_x is one of the major air pollutants coming from exhaust gases of various combustion processes and NO_x removal remains one of the most challenging tasks for the researchers. Gold catalysts based on appropriate metal oxide supports could be used successfully as TWCs during the "cold start". There are data in the literature on the activity of gold-based catalysts in NO reduction by CO, hydrogen or hydrocarbons [13–16]. Recently, Bera et al. [17,18] have applied Ag and Au supported on ceria as active combustion catalysts. Our previous studies have shown that gold-based catalysts on ceria and ceria–alumina are very promising for NO reduction by CO [10–12]. These catalysts exhibited high activity with 100% selectivity to N_2 at 200 °C. It was established also that the formed oxygen vacancies play a decisive role for higher activity by increasing the oxygen mobility. Another advantage of these catalysts consisted in the high activity exhibited in WGS reaction [5,6]. The produced hydrogen in the presence of water additionally favored the reduction of NO by CO [11,12].

The aim of this paper is to synthesize highly active, selective and stable gold catalysts supported on ceria modified by rare earth metals (Y, La, Sm and Gd). The mixed oxide supports are prepared by co-precipitation technique. The influence of the nature of the modifiers on the structure and reactivity of gold catalysts will be discussed. Special attention should be addressed on the role of oxygen vacancies created upon addition of Me^{3+} dopants.

* Corresponding author.
E-mail address: luilieva@ic.bas.bg (L. Ilieva).

0920-5861/$ – see front matter © 2008 Elsevier B.V. All rights reserved.
doi:10.1016/j.cattod.2008.06.033

2. Experimental

2.1. Samples preparation

The mixed CeO_2–Me_2O_3 (Me = Y, La, Sm, and Gd) supports were prepared by co-precipitation technique from a solution of the corresponding metal nitrates in appropriate ratio (the amount of Me_2O_3 was 10 wt%) with a solution of K_2CO_3 at constant pH 9.0 and temperature 60 °C. The resulting precipitates were aged at the same temperature for 1 h, then filtered and washed until removal of NO_3^- ions. The washed precipitates were dried in vacuum at 80 °C and calcined under air at 400 °C for 2 h. Gold (2 wt%) was added by deposition–precipitation method. It was loaded as $Au(OH)_3$ on the corresponding mixed metal oxide support, preliminary suspended in water. The precipitation was carried out in a "Contalab" system (Switzerland) under full control of all parameters of preparation (pH, temperature, stirring speed, reactant feed flow rates, etc.). The details are given in Ref. [6]. After filtering and careful washing, the precursors were dried under vacuum and calcined in air at 400 °C for 2 h. The samples were denoted as AuCeY, AuCeLa, AuCeSm and AuCeGd. All the initial salts used were "analytical grade".

2.2. Sample characterization

The BET surface area of the samples was determined with a Micromeritics 'Flow Sorb II-2300' device with 30% N_2, 70% He mixture at atmospheric pressure and N_2 liquid temperature.

The X-ray diffraction patterns were obtained with a DRON-3 automatic powder diffractometer, using Cu $K\alpha_1$ radiation. The crystal size of ceria particles was calculated on the basis of the peak broadening using "Powder Cell" program. The program gives the possibility of fitting the experimental XRD spectra, based on the corresponding theoretical structures. The instrumental broadening effect was taken into consideration. The XRD profiles were approximated by Lorentz functions.

The Raman spectra were recorded using a SPEX 1403 double spectrometer with a photomultiplier, operating in the photon counting mode. The 488 nm line of an Ar^+ ion laser was used for excitation. The laser power on the samples was 10 mW. The samples were prevented from overheating during the measurements by increasing the size of the focused laser spot. The optimal conditions were chosen by checking the intensity, position and the width of the 464 cm^{-1} Raman line of CeO_2. The spectral slit width was 4 cm^{-1}.

The TPR measurements were carried out by means of an apparatus described elsewhere [19]. A cooling trap (−40 °C) for removing the water formed during reduction was mounted in the gas line prior to the thermal conductivity detector. A hydrogen–argon mixture (10% H_2), dried over a molecular sieve 5A (−40 °C), was used to reduce the samples at a flow rate of 24 ml min^{-1}. The temperature was linearly raised at a rate of 15 °C min^{-1}. The charged sample mass was 0.05 g. It was selected based on the criterion proposed by Monti and Baiker [20]. In addition, consecutive TPR experiments were carried out after re-oxidation with purified air at the temperature, immediately after the end of the first TPR peak (220 °C) of the fresh sample. The H_2–Ar flow was switched over to air flow for 15 min and the new TPR pattern was recorded after cooling down to room temperature in purified helium. The hydrogen consumption (HC) during the reduction processes was calculated using preliminary calibration of the thermal conductivity detector, performed by reducing different amounts of NiO to Ni (NiO – "analytical grade" of purity, calcined for 2 h at 800 °C to avoid the presence of non-stoichiometric oxygen).

2.3. Catalytic activity measurements

The catalytic test of NO reduction by CO was performed using a quartz glass U-shaped reactor, equipped with a temperature programmed controller. The reactants and products were monitored by ABB IR and UV analysers. The QM (quadrupole mass) analysis of the reaction products including ammonia and methane was also performed using on-line Pfeiffer quadrupole mass spectrometer and Balzers Quadstar software. The conversion degree of NO and CO was taken as a measure of catalytic activity. The steady-state tests were made upon increasing the reaction temperature, waiting at each temperature for a constant conversion value. The catalysts were tested in a wide temperature interval charging 0.05 g of the sample at a flow rate of 50 ml min^{-1} corresponding to WHSV of 60,000 ml g^{-1} h^{-1}. The pretreatment of the catalyst was provided according to the previously chosen conditions [10–12] using 5% H_2 in argon for 30 min at 120 °C. The corresponding reaction mixture was prepared using pure He as a rest. The catalysts stability was tested keeping the sample at reaction conditions for 19 h at 200 °C and 3 h at 400 °C. The selectivity to N_2 was calculated from the difference between the initial NO and the other possible N containing products monitored during the reaction.

3. Results

3.1. Catalysts characterization

The BET surface area, lattice parameters and average particle size of ceria, estimated by XRD, are given in Table 1. The data for gold supported on not modified ceria [6] are also given. With respect to the corresponding initial supports, the addition of gold leads to an increase of the BET surface area suggesting deposition of very small gold particle.

The X-ray diffraction spectra are represented in Fig. 1. The lack of gold metal reflections suggests the presence, if any, of Au crystallites size smaller than the detection limit of 2–3 nm. The average size of gold for AuCe catalyst, estimated by HRTEM [21] was indeed 2.0 nm. The data showed that ceria supports are also nano-structured having average particle sizes <10 nm. Concerning the lattice parameter *a*, a higher value for the La containing sample was obtained as compared to AuCe, while a smaller value was obtained for the Y containing sample. In the case of Sm and Gd modifiers, the *a* parameters were close to that of AuCe sample.

Table 1
BET surface area, lattice parameters and average size of ceria particles

Samples	S_{BET} (m^2 g^{-1})	Ionic radius of Me^{3+} dopants (Å)	Lattice parameter of ceria[a] *a* (Å)	Average size of ceria (nm)
AuCe	108 (84)	–	5.422	8.0
AuCeLa	81 (55)[b]	1.161	5.451	6.3
AuCeSm	84 (54)	1.079	5.421	7.1
AuCeGd	78 (53)	1.053	5.422	6.8
AuCeY	103 (54)	1.019	5.416	6.9

[a] Lattice parameter of CeO_2 = 5.412 Å.
[b] Values in parentheses corresponding to the initial supports.

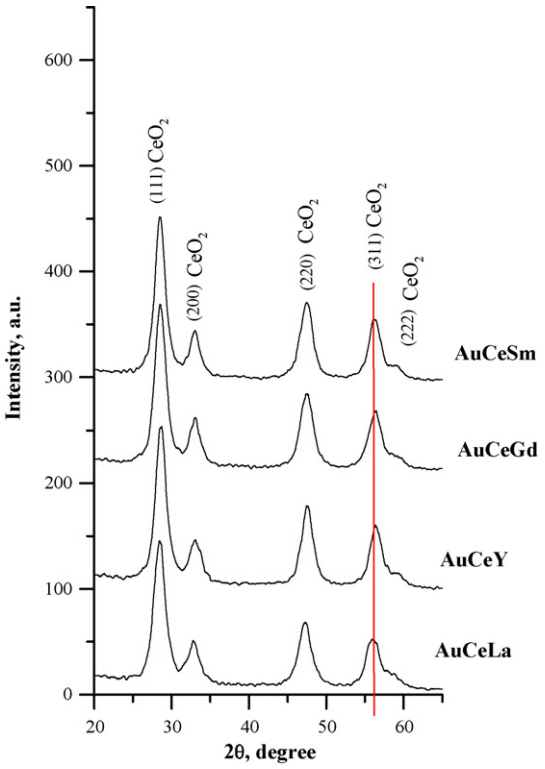

Fig. 1. XRD profiles of the studied catalysts.

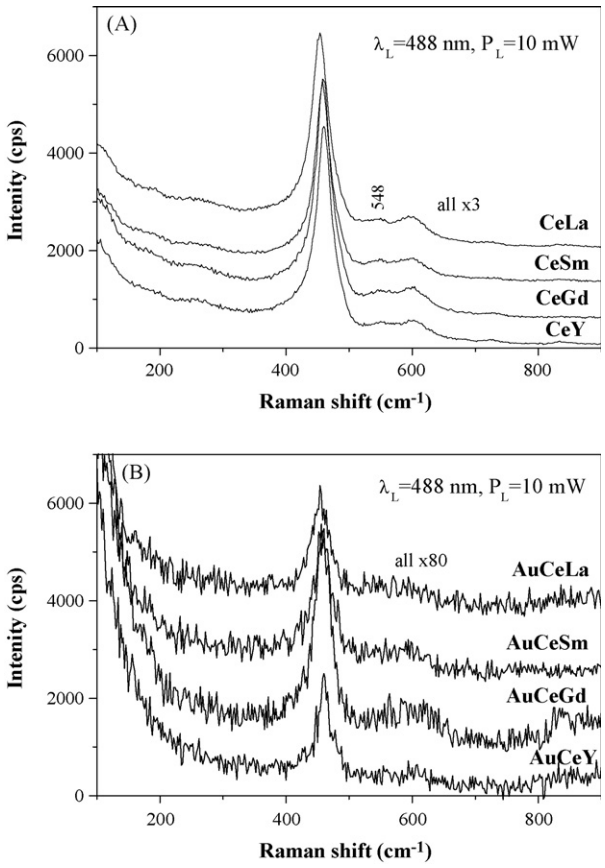

Fig. 2. Raman spectra of the initial supports (A) and gold containing samples (B).

Raman spectra of the studied catalysts are presented in Fig. 2: initial supports (Fig. 2A) and after deposition of gold (Fig. 2B). The addition of gold makes the samples strongly absorbing. It results in a decrease of the peaks intensities. The main line of CeO_2 dominates in the spectra. A weak line at 548 cm^{-1} was also observed. In a study of ceria doped by different lanthanides, McBride et al. have attributed a broad feature near 570 cm^{-1} to oxygen vacancies created in the ceria structure [9]. The full width at the half of maximum (FWHM) of the main line was calculated and the data are presented in Table 2. In the same table the FWHM value for gold supported on unmodified ceria (AuCe) [10] is also given. It is seen, that the addition of Me^{3+} leads to an increase in the FWHM values for both the initial supports and the gold catalysts. The increase in this value is different depending on the modifier.

In Fig. 3 the low temperature (LT) TPR profiles of the studied gold catalysts, after direct reduction (A) and after reoxidation (B) are shown. The registered LT TPR peaks are due to the reduction of surface layers of ceria and oxygen species around small gold particles [5,6]. A symmetric TPR peak with T_{max} = 103 °C was recorded in the case of the fresh AuCeY sample. For AuCeGd and AuCeLa identical patterns with T_{max} = 108 °C were obtained. They are asymmetric with a high temperatures (HT) tail. The lowest T_{max} = 94 °C was observed for AuCeSm, the peak is obviously complex. After reoxidation all TPR peaks are broader and less intense and they are located within the lower temperature interval than the TPR peaks of the corresponding fresh samples. The quantitative comparison of the peak intensities, in view of oxygen storage capacity of the catalysts can be obtained from the calculated HC, given in Table 3. In the same table the data of AuCe catalyst [10] are also presented. For all gold samples supported on ceria doped by Me^{3+} the HC was higher than that of AuCe, the highest one being for AuCeY sample. After reoxidation the oxygen capacity was not fully recovered and it remained lower as compared to the fresh samples. In the case of Y containing

Table 2
Full width at half maximum (FWHM) of the dominant ceria line in the Raman spectra

Support Au-catalysts	Initial supports FWHM (cm^{-1})	Gold catalysts FWHM (cm^{-1})
Ce/AuCe	12.0	13.5
CeLa/AuCeLa	32.8	32.0
CeSm/AuCeSm	30.0	32.2
CeGd/AuCeGd	29.7	31.0
CeY/AuCeY	30.9	29.2

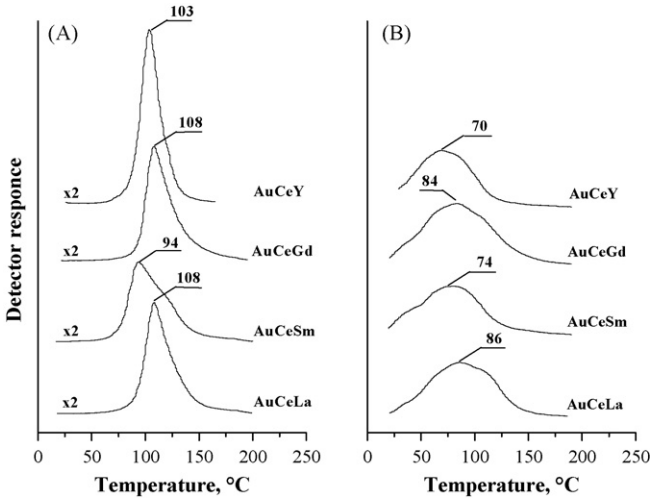

Fig. 3. TPR patterns of fresh samples (A) and after reoxidation (B).

Table 3
Hydrogen consumption in the LT interval concerning direct TPR and TPR after re-oxidation

Sample	Direct TPR		TPR after reoxidation	
	HC (μmol g^{-1})	Degree of reduction (%)	HC (μmol g^{-1})	Degree of reduction (%)
AuCe	462	16.9	304	10.5
AuCeLa	598	22.9	366	14.0
AuCeSm	598	22.9	382	14.6
AuCeGd	598	22.9	378	14.5
AuCeY	690	26.4	272	10.4

sample the biggest difference in HC of fresh and reoxidized sample was observed. Based on the stoichiometric amount of hydrogen for the reduction $CeO_2 \rightarrow Ce_2O_3$ (2904 μmol g^{-1} calculated for CeO_2 and 2614 μmol g^{-1} – for CeO_2 doped by 10 wt% Me_2O_3), the corresponding degree of reduction for each sample is also given in Table 3. According to literature data the reduction of ceria limited to surface layer processes is 17% [22] or 20% as reported in Ref. [23]. In our case we assigned the calculated degree of reduction to the surface layer processes because a small amount of hydrogen could be retained in the bulk of ceria [23–25].

3.2. Catalytic activity measurements

The catalytic activity of the studied gold catalysts on doped ceria was estimated in the reduction of NO by CO under different conditions: (1) using a feed composition: 3000 ppm NO + 3000 ppm CO + 3000 ppm H_2 and (2) in the presence of water: 1500 ppm NO + 3000 ppm CO + 1000 ppm H_2 + 5% H_2O. These conditions were chosen on the basis of our previous investigation on Au supported on ceria–alumina [10]. The catalytic activity results of AuCeSm and AuCeLa catalysts concerning the 1st experimental route are represented in Fig. 4(A) and (B). Some small amount of NO was converted to N_2O only at temperatures up to 150 °C. At 200 °C QM monitoring showed that a jump in NH_3 formation rate occurs and a small amount of CH_4 starts to be registered for both samples. Fig. 5(A) illustrates the QM signals in the case of AuCeSm catalyst. Concerning the 2nd experimental route, the results of the catalytic activity measurements of AuCeSm, AuCeLa, AuCeGd and AuCeY samples are shown in Fig. 6(A–D). Again a low amount of N_2O was registered below 150 °C. However, the QM analysis showed that a significant improvement of the selectivity toward N_2 was achieved—neither NH_3 nor CH_4 were formed at temperatures up to 400 °C for all studied samples. QM signals in the case of AuCeSm catalyst are presented in Fig. 5(B). In the presence of water, the catalytic activity data on Sm, Gd and La containing samples were very

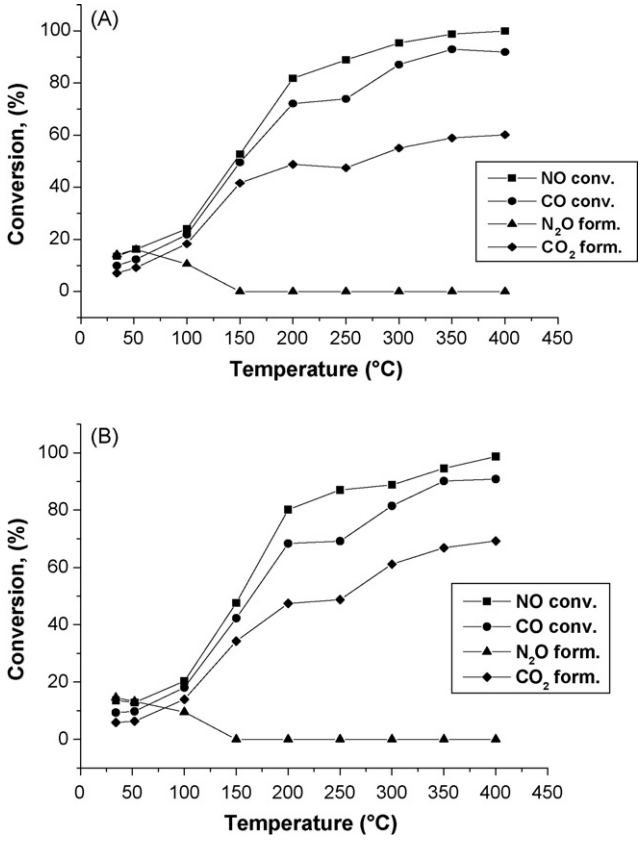

Fig. 4. Catalytic activity results in NO reduction by CO using gas feed 3000 ppm NO + 3000 ppm CO + 3000 ppm H_2: AuCeSm (A) and AuCeLa (B).

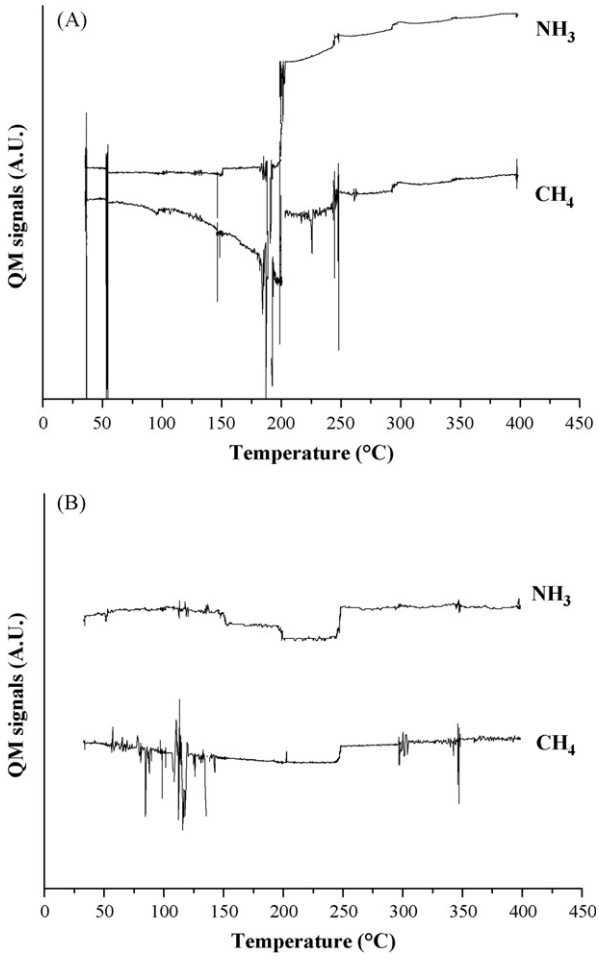

Fig. 5. QM signals of NH_3 and CH_4 during the catalytic tests of AuCeSm sample: 1st experimental route (A) and 2nd experimental route (B).

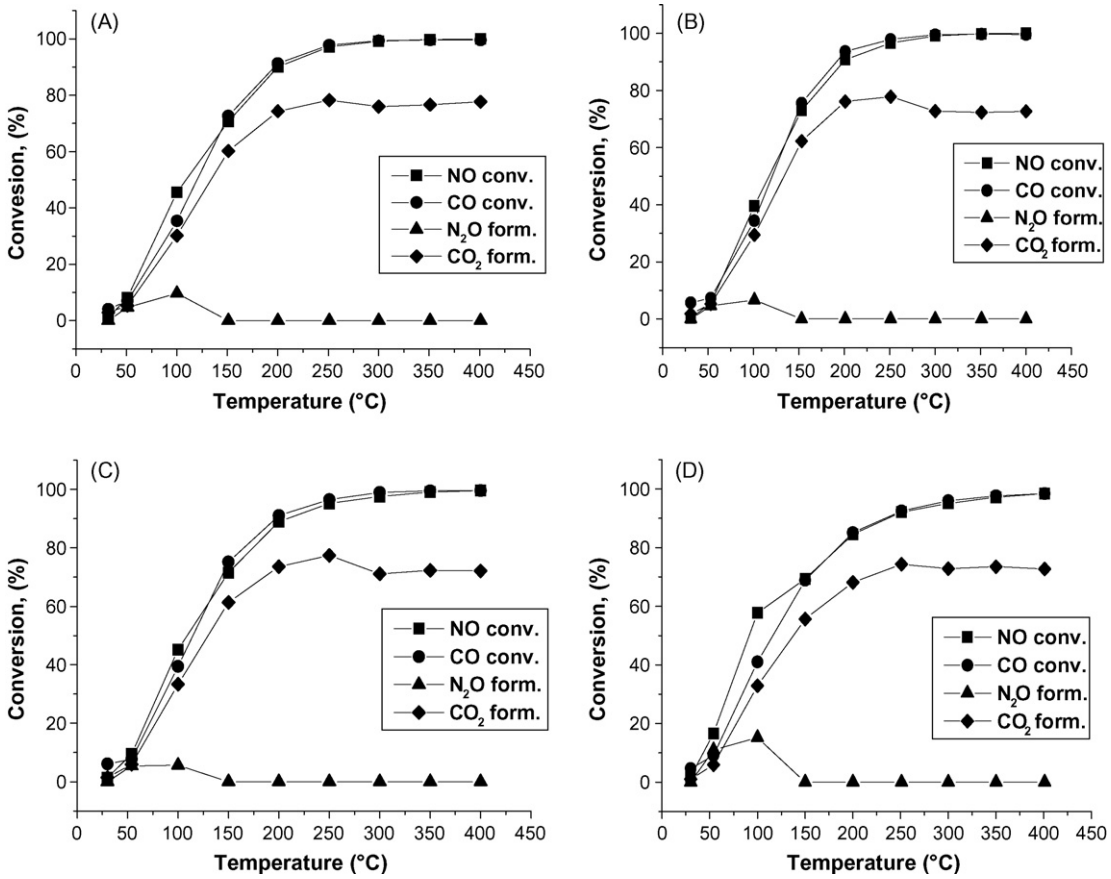

Fig. 6. Catalytic activity in NO reduction by CO using gas feed 1500 ppm NO + 3000 ppm CO + 1000 ppm H_2 + 5% H_2O: AuCeSm (A); AuCeLa (B); AuCeGd (C); AuCeY (D).

similar, a slightly higher NO and CO conversion was observed for AuCeSm sample. On the contrary, the activity of the AuCeY sample was lower compared to the catalysts with lanthanides. The test of stability, performed on the AuCeSm sample after 2nd experimental route showed that after a long catalytic operation of 19 h at 200 °C, the sample lost only 1% of the activity. During the subsequent 3 h stability test at 400 °C the activity practically was not changed.

4. Discussion

Our previous study of NO reduction by CO has shown that the enhanced oxygen vacancy formation due to the presence of Al^{3+} in the mixed CeO_2–Al_2O_3 support correlates with the activity over corresponding supported gold catalysts in this reaction [10–12]. It is known [4] that the structure of the fluorite assembly tolerates a high level of atomic disorder upon doping ceria with Me^{3+} ions. The crystal lattice must compensate for the excess negative charge by three mechanisms: vacancy compensation, cerium interstitial compensation and dopant interstitial compensation [4]. For smaller cations (as Al^{3+}) the vacancy compensation is accompanied by some compensation via dopant interstitial, while in the case of Me^{3+} dopants with radius >0.8 Å, the vacancy compensation is the preferred route [4].

The deposition of gold on ceria causes a strong modification, resulting in the creation of oxygen vacancies and Ce^{3+} [6,26]. As the ionic radius of Ce^{3+} (1.14 Å) is higher than that of Ce^{4+} (0.97), the generated Ce^{3+} leads to an increase in the lattice parameter of ceria. In the case of CP technique of preparation, applied in the present study, the substitution of Ce^{4+} by Me^{3+} dopant determines the formation of oxygen vacancies deeply into the bulk of ceria. It leads to a change in the lattice parameter *a* in accordance with the ionic radius of the corresponding dopant. The larger or the smaller dopants will expand or contract the lattice, respectively. Indeed, a highest increase of *a* value is observed in the case of La, the lowest one – in the case of Y. The calculated values for AuCeSm and AuCeGd are quite similar because of the close values of their ionic radii. The presence of the studied dopants strongly influences the FWHM values of the main ceria line in the Raman spectra. The FWHM value depends on ceria dispersion as well as on the defects in ceria lattice, including oxygen vacancies [27,28]. The introduction of Me^{3+} dopants causes an increase in the FWHM values with respect to non-promoted ceria. Since the average size of ceria was similar for all the samples, the widening is likely to be connected to the formation of oxygen vacancies in ceria upon the addition of Me^{3+}. The comparison between FWHM values of the initial supports and those of gold catalysts shows a small decrease after deposition of gold in the case of La doping. The presence of Y causes a bigger decrease, while in the case of Sm and Gd containing samples, the deposition of gold leads to an increase of the FWHM value. The results show that both gold and modifiers influence the structure of ceria, the effects being complicate and depending on the ionic radius and nature of the Me^{3+} dopant.

Comparing only the TPR profiles of fresh gold catalysts, as it is usually done by many authors using TPR for catalysts characterization, it could be concluded that in the present study there is no correlation between reducibility and catalytic activity, especially in the case of Y as a dopant. The AuCeY sample exhibits the lowest activity although it appears the most reducible. However, comparing the results after reoxidation of the samples, a reverse behaviour is observed with the least reducible being AuCeY. The

results are also in agreement with the lowest FWHM value of AuCeY catalyst, e.g. less defective structure compared to ceria doped by the lanthanides. The HCs for the gold catalysts containing La, Sm and Gd are slightly different, a little higher is the HC for the AuCeSm sample. It is worth noticing that the reoxidation temperature was chosen into the interval of interest for the test reaction of NO + CO. The LT reducibility of the reoxidized gold catalysts supported on doped CeO_2 showed a good correlation with their catalytic properties. The degrees of NO and CO conversion for the lanthanides containing gold catalysts are quite close, the AuCeSm sample being slightly more active. It has been reported that the CeO_2–Sm_2O_3 system, among the doped-ceria materials, exhibits the highest electrical conductivity since Sm^{3+} doping induces the least distortion of the parent lattice [29].

The test of stability showed a stable CO and NO conversion during a long period of catalytic operation at 200 °C. Moreover, the overheating up to 400 °C did not affect the catalytic behaviour.

The selectivity to N_2 depends on the feed gas composition. In the absence of water, NH_3 as well as CH_4 formation start at 200 °C (Fig. 4(A)). This behaviour is different from the case of Au/CeO_2–Al_2O_3 catalysts, prepared by the same method of co-precipitation [10]. Under similar experimental conditions higher selectivity was observed over gold catalysts supported on mixed ceria–alumina carriers. Ammonia was registered above 220 °C and no CH_4 trace was observed into the considered temperature interval. For Au/CeO_2–Al_2O_3 samples the same results concerning the selectivity to N_2 were found adding water to the gas feed [12]. However, in the case of gold supported on ceria doped by the rear earth Me^{3+}, the addition of water leads to a substantial improvement of the selectivity—in the entire studied temperature interval no NH_3 and no CH_4 formation was recorded. The degrees of NO and CO conversion are comparable for both ceria doped by aluminum or by lanthanides. Since moisture is generally present in the real exhaust gases, the results obtained in this study show that gold catalysts on lanthanides doped ceria exhibit better performance in the reaction of NO reduction by CO in comparison to the gold catalysts on ceria modified by Al^{3+}.

5. Conclusions

Gold catalysts, supported on lanthanides doped ceria, were synthesized and they showed high activity and stability in NO reduction by CO. Conversions both of NO and CO at 250 °C were close to 100% using Sm, La or Gd as dopants. Below 250 °C the Au catalyst on Sm doped ceria exhibited slightly higher activity. The lowest catalytic activity was observed using Y as a modifier.

The introduction of Me^{3+} dopants into ceria caused a change in the lattice parameter *a*, correlated with the ionic radius of the dopant. No substantial influence of the average size of ceria crystallites was found by XRD technique. A higher amount of oxygen vacancies compared to undoped ceria were formed according to the data of Raman spectroscopy and TPR. The LT reducibility of the reoxidized gold catalysts supported on doped CeO_2 showed a good correlation with their catalytic properties.

It was established that the addition of water to the feed gas improved the catalysts selectivity to N_2. The 100% selectivity within the temperature interval 150–400 °C in the presence of water makes these gold catalysts promising for practical application.

Acknowledgments

This research study has been performed in the framework of a D36/003/06 COST program and a NATO grant CBP.EAP.CLG982799. L.I., I.I., R.N. and D.A. gratefully acknowledge the support by National Science Fund, Ministry of Education and Sciences of Bulgaria (project X-1502). The authors thank Prof. K. Petrov for the assistance and helpful comments concerning XRD results.

References

[1] T. Bunluesin, R.J. Gorte, Appl. Catal. B: Environ. 15 (1998) 107.
[2] T. Shido, Y. Iwasawa, J. Catal. 141 (1993) 71.
[3] J.Z. Shyu, K. Otto, W.L.H. Watkins, G.W. Graham, R.K. Belitz, H.S. Gandhi, J. Catal. 23 (1988) 114.
[4] A. Trovarelli, Catal. Rev. Sci. Eng. 38 (1996) 439.
[5] D. Andreeva, V. Idakiev, T. Tabakova, L. Ilieva, P. Falaras, A. Bourlinos, A. Travlos, Catal. Today 72 (2002) 51.
[6] D. Andreeva, I. Ivanov, L. Ilieva, J.W. Sobczak, G. Avdeev, K. Petrov, Top. Catal. 44 (2007) 173.
[7] Y. Zhang, S. Anderson, M. Muhammed, Appl. Catal. B: Environ. 6 (1995) 325.
[8] A.E.C. Palmqvist, E.M. Johansson, S.G. Jaras, M. Muhammed, Catal. Lett. 56 (1998) 69.
[9] J.R. McBride, K.C. Hass, B.D. Poindexter, W.H. Weber, J. Appl. Phys. 76 (1994) 2435.
[10] L. Ilieva, G. Pantaleo, I. Ivanov, A.M. Venezia, D. Andreeva, Appl. Catal. B: Environ. 65 (2006) 101.
[11] L. Ilieva, G. Pantaleo, J.W. Sobczak, I. Ivanov, A.M. Venezia, D. Andreeva, Appl. Catal. B: Environ. 76 (2007) 107.
[12] L. Ilieva-Gencheva, G. Pantaleo, N. Mintcheva, I. Ivanov, A.M. Venezia, D. Andreeva, J. Nanosci. Nanotechnol. 8 (2008) 867.
[13] A. Ueda, M. Haruta, Gold Bull. 32 (1999) 3, and references therein.
[14] M.C. Kung, J.-H. Lee, H.H. Kung, Am. Chem. Soc., Div. Fuel Chem. 40 (1995) 1073.
[15] M.A.P. Dekkers, M.J. Lippits, B.E. Nieuwenhuys, Catal. Today 54 (1999) 381.
[16] J.R. Mellor, A.N. Palazov, B.S. Grigorova, J.F. Greyling, K. Reddy, M.P. Letsoalo, J.H. Marsh, Catal. Today 72 (2002) 145.
[17] P. Bera, K.C. Patil, M.S. Hedge, PCCP 2 (2000) 3715.
[18] P. Bera, M.S. Hedge, Catal. Lett. 79 (2002) 75.
[19] N. Kotzev, D. Shopov, J. Catal. 22 (1971) 297.
[20] D.A.M. Monti, A. Baiker, J. Catal. 83 (1983) 323.
[21] T. Tabakova, F. Boccuzzi, M. Manzoli, J.W. Sobczak, V. Idakiev, D. Andreeva, Appl. Catal. A 298 (2006) 127.
[22] M.G. Sanchez, J.L. Gazquez, J. Catal. 104 (1987) 120.
[23] A. Laachir, V. Perrichon, A. Bardi, J. Lamotte, E. Catherine, J.C. Lavalley, J. El Faallah, L. Hilaire, F. le Normand, E. Quemere, G.N. Sauvion, O. Touret, J. Chem. Soc., Faraday Trans. 87 (1991) 1601.
[24] L. Ilieva, G. Pantaleo, G. Munteanu, A.M. Venezia, D. Andreeva, Rev. de Roum. Chim. 52 (2007) 975.
[25] J.L.G. Fierro, J. Soria, J. Sanz, J.M. Rojo, J. Solid State Chem. 66 (1987) 154.
[26] T. Tabakova, F. Boccuzzi, M. Manzoli, D. Andreeva, Appl. Catal. A: Gen. 252 (2003) 385.
[27] G.W. Graham, W.H. Weber, C.R. Peters, R. Usmen, J. Catal. 130 (1991) 310.
[28] I. Kosacki, T. Suzuki, H.U. Anderson, Ph. Colomban, Solid State Ionics 149 (2002) 99.
[29] Y. Wang, T. Mori, J.-G. Li, Y. Yajima, Sci. Technol. Adv. Mater. 4 (2003) 229, and references therein.